Advanced TiC/a-C:H nanocomposite coatings deposited by magnetron sputtering

Y.T. Pei [a,*], D. Galvan [a], J.Th.M. De Hosson [a], C. Strondl [b]

[a] *Department of Applied Physics, Materials Science Center and Netherlands Institute for Metals Research, University of Groningen, Nijenborgh 4, 9747 AG Groningen, The Netherlands*
[b] *Hauzer Techno Coating BV, van Heemskerckweg 22, 5928 LL Venlo, The Netherlands*

Available online 9 August 2005

Abstract

TiC/a-C:H nanocomposite coatings have been deposited by magnetron sputtering. They consist of 2–5 nm TiC nanocrystallites embedded in the amorphous hydrocarbon (a-C:H) matrix. A transition from a columnar to a glassy microstructure has been observed in the nanocomposite coatings with increasing substrate bias or carbon content. Micro-cracks induced by nanoindentation or wear tests readily propagate through the column boundaries whereas the coatings without a columnar microstructure exhibit substantial toughness. The nanocomposite coatings exhibit hardness of 5–20 GPa, superior wear resistance and strong self-lubrication effects with a friction coefficient of 0.05 in air and 0.01 in nitrogen, under dry sliding against uncoated bearing steel balls. Especially, reversible transitions from low to ultra-low friction are observed if the atmosphere is cycled between ambient air and nitrogen. The lowest wear rate is obtained at high humidity.
© 2005 Elsevier Ltd. All rights reserved.

Keywords: Films; Nanocomposites; Wear resistance; TiC/a-C:H; Engine components

1. Introduction

Nanocomposite coatings consisting of nanocrystalline ceramic particles embedded in an amorphous hydrocarbon (a-C:H) matrix are able to combine high fracture toughness and wear resistance with a low friction coefficient. These combined properties are attractive for applications on drive-line components in the automotive industry. In such applications, a wear resistant coating must support high loads under sliding or rolling contact without failure by cohesive fracture, or loss of interfacial adhesion. Most frequently, a low friction coefficient is required, which helps to reduce friction losses and to increase load support capability. The latter is evident from the fact that typical coating failures such as cracking, chipping and delamination are primarily caused by the tangential stress that is proportional to the contact load through the friction coefficient. Only recently it has been possible to realize all of these requirements in nanostructured or nanocomposite coatings. An example of these a-C(:H) based nanocomposite coatings is the TiC/a-C:H system,[1] in which a correlation between coating mechanical properties and metal concentration has been made by Meng et al.[2,3]

Although the microstructure and mechanical properties, such as the Young's modulus and hardness, of TiC/a-C:H nanocomposite coatings have been studied in some detail, less information exists in literature on the correlation between the coating microstructure, the mechanical properties, and the macroscopic tribological characteristics. In this paper, we report on the deposition and characterization of TiC/a-C:H nanocomposite coatings. The tribological behavior of the nanocomposite coatings is scrutinized in conjunction with the detailed examinations of the mechanical properties. Cross-sectional and planar TEM observations and energy filtered TEM are employed to characterize the nanostructure and the element distribution in the coatings. The influence of the volume fraction and size distribution of nanocrystallites TiC (nc-TiC) on the coating properties has been examined.

* Corresponding author. Tel.: +31 50 363 4344; fax: +31 50 363 4881.
 E-mail address: y.t.pei@phys.rug.nl (Y.T. Pei).

2. Experimental

TiC/a-C:H nanocomposite coatings were deposited with closed-field unbalanced magnetron sputtering in an argon/acetylene atmosphere in a Hauzer HTC-1000 coating system, which was configured of two Cr targets and two Ti targets opposite to each other. The detailed set-up of the coating system has been documented elsewhere.[4] The Cr targets were used to create an intermediate layer between the nc-TiC/a-C:H coating and the substrate material. The flow rate in standard cubic centimeters per minute (sccm) of acetylene and substrate bias varied in the range of 80–125 sccm and 0–150 V, respectively, to obtain different C/Ti contents and nanostructures in the coatings. The substrates used for each coating were Ø 30 mm × 5 mm discs of hardened M2 steel, 304 stainless steel and Ø 100 mm Si wafer for the measurements of residual stress by monitoring the curvature change.

A calibrated MTS Nano Indenter XP was employed to measure the hardness (*H*) and Young's modulus (*E*) of the coatings with a Berkovich indenter and the fracture toughness with a cube-corner indenter according to Lawn–Evans–Marshall's approach.[5,6] In order to have a reliable statistic, 30 indentations in total were configured on three different areas of each coating sample. The maximum indentation depth for measuring *H* and *E* was fixed at one tenth of the coating thickness, namely 150 nm. The averaged *H* and *E* values over the range of depth of 60–150 nm were taken as the hardness and modulus for a coating.

Tribo-tests were performed on a CSM tribometer with a ball-on-disc configuration at 0.1 m/s sliding speed and 2 N or 5 N normal load. Only the coatings deposited on hardened M2 steel discs in dimensions of Ø 30 mm × 5 mm were tested, sliding against uncoated Ø 6 mm 100Cr6 steel ball or alumina ball. The radius of the wear tracks was set in the range of 10–14 mm with an interval of 1 mm between the tracks. Different levels of humidity were achieved by flowing water vapor or dry nitrogen in the testing chamber at least for 45 min before a wear test. A confocal microscope was used to capture 3D images on a wear track for measuring the wear volume and then to calculate the wear rate of a coating. In the ball-on-disc configuration an area of the ball is in contact with the coating all the time, whereas the corresponding areas on the coating are only in contact once a lap or revolution. The total sliding distance made in a tribo-test is thus only

relevant to the ball and is meaningless for the coating. Actually, the laps or revolutions run in a test are more essential to the coating sample, no matter how large the diameter of the wear tracks. Therefore, the wear rate (*W*r) of the coatings is defined as volume of wear per unit track length, per Newton of normal load and per lap. Even though the calculated value of the wear rate according to this definition is exactly the same as that calculated from the total sliding distance of the ball (equal to the product of laps and perimeter of the wear track), its physical meaning is different from the commonly used dimension "mm³/Nm" of wear rate that only counts for the configuration of a coated ball sliding against a disc as the reference material.

The surface morphology and fractured cross sections of the coatings were examined using a scanning electron microscope (Philips FEG-XL30s). The investigation of the nanostructures was carried out in a high-resolution transmission electron microscope (HR-TEM) (JEOL 4000 EX/II, operated at 400 kV) and an analytical TEM (JEOL 2010F-FEG, operated at 200 kV). Electron probe microanalysis (EPMA) with a Cameca SX-50 equipment was used to determine the chemical composition of the coatings.

3. Results and discussion

Table 1 summarizes the deposition parameters, chemical compositions and mechanical properties of the nc-TiC/a-C:H nanocomposite coatings. A pure chromium intermediate layer with a thickness of about 100 nm has been deposited first for all the coatings to enhance the interfacial adhesion to the substrates. The Cr layer is followed by a 100 nm thick transition layer, in which the chromium content gradually decreases to zero and the titanium concentration continuously increases to 100%. Then acetylene gas is introduced to deposit each nanocomposite layer with the desired composition. Changes in the flow rate of acetylene gas lead to a variation of the carbon content in the nanocomposite coatings as expected.

SEM micrographs presented in Fig. 1 show the fractured cross-sections of the nanocomposite coatings. Both the intermediate layer and the transition layer are characterized by columnar structures in all the coatings. In contrast, a clear evolution from columnar to glassy microstructure in the nanocomposite layers is observed with increasing substrate

Table 1
Deposition parameters, composition and properties of nc-TiC/a-C:H nanocomposite coatings

| Coating no.	C$_2$H$_2$ (sccm)	Bias (−V)	Composition[a] (at.%)			*H* (GPa)	*E* (GPa)	*H/E*	Toughness (MPa m$^{1/2}$)	*L*$_r$ (mN)	*W*$_e$/*W*$_t$
			C	Ti	O						
H1	110	Floating	71.34	13.64	15.02	5.5	61.3	0.091	–	–	–
H2	110	60	80.21	16.33	3.46	11.8	99.8	0.118	23.66	80	0.2449
H3	110	100	81.02	17.84	1.14	15.6	136.6	0.114	36.15	90	0.2697
H4	110	150	80.30	18.51	1.19	19.8	168.3	0.118	49.94	220	0.2903
H5	80	100	66.60	31.75	1.65	20.0	229.4	0.087	32.21	60	0.2639
H6	125	100	87.19	11.85	0.96	15.8	128.5	0.123	55.78	200	0.2814

[a] Excluding hydrogen.
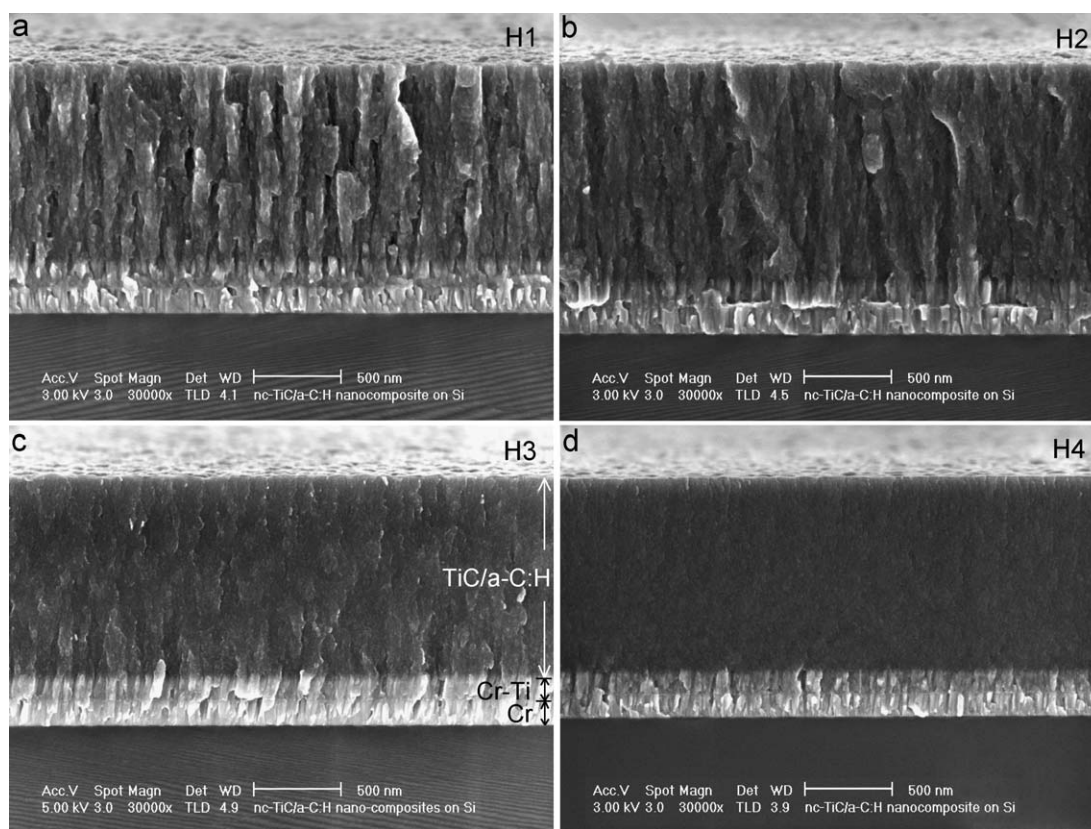
Fig. 1. SEM micrographs showing the fractured cross-sections of nanocomposite coatings deposited at 110 sccm flow rate of acetylene gas and different substrate bias: (a) floating, (b) −60 V, (c) −100 V and (d) −150 V.

bias. The columnar microstructure in the coating H2 (Fig. 1b) gets slightly weaker compared with that in the coating H1 sputtered at floating bias (Fig. 1a), and is hardly traceable in the coating H3 deposited at 100 V bias (Fig. 1c). Increasing the substrate bias further to 150 V, the coatings become harder and are free from columnar growth. Consequently, the fractured cross sections of the coating H4 appear flat and show only some contrast of exposed nanoparticles as shown in Fig. 1d. A similar transition from columnar to glassy microstructure is also observed to respond to an increase in carbon content, i.e. in the coatings from H5, H3 to H6.

High resolution TEM presented in Fig. 2 clearly reveals that the nanocrystalline TiC particles are homogeneously embedded in the a-C:H matrix and an increase in Ti content leads to the formation of bigger TiC particles, e.g. 2 nm versus 5 nm in diameter observed in the two coatings H3 and H5 consisting of 17.84 at.% and 31.75 at.% Ti, respectively. Indexing the lattice fringes and also the circular selected area diffraction patterns confirms the formation of TiC nanocrystalline phases.

Nanoindentation was employed to measure the hardness (H) and Young's modulus (E) of the coatings with a Berkovich indenter. As seen in Table 1, increasing substrate bias leads to a clear increase in both the hardness (H) and elastic modulus (E) of the nanocomposite coatings. However, the H/E ratio stays almost constant when the substrate bias is equal to

and above 60 V. On the other hand, higher flow rate of acetylene gas, i.e. higher C-content, results in markedly higher H/E ratios, which is analogous to the results obtained in the nc-TiC/a-C nanocomposite coatings.[7] The highest H/E ratio of 0.123 is achieved on the coating H6 with 87 at.% C. Although for a long time hardness has been regarded as a primary material property affecting wear resistance, the elastic strain to failure, which is related to the H/E ratio, is a more suitable parameter for predicting wear resistance.[8] Within a linear-elastic approach, this is understandable according to the relations that the yield stress of contact is proportional to (H^3/E^2) and the equation $G_c = \pi a \sigma_c^2 / E$, indicating that the fracture toughness of coatings defined by so-called 'critical strain energy release rate' G_c would be improved by both a *low* Young's modulus and a *high* critical stress (σ_c) for fracture which implies a need for high hardness. Indeed, the significance of the H/E ratio in wear control reflects in the wear behavior of the nanocomposite coatings as to be discussed later in this section.

Attempts in the use of nanoindentation to quantify the fracture toughness were also made in this work, but the approach seemed not really applicable on supertough coatings like the nanocomposite coatings reported here. Although the indentation depth (2.1–2.4 μm) made at maximum load of 190 mN with a cube-corner indenter has already exceeded the thickness of all the coatings, the radial cracks formed on the
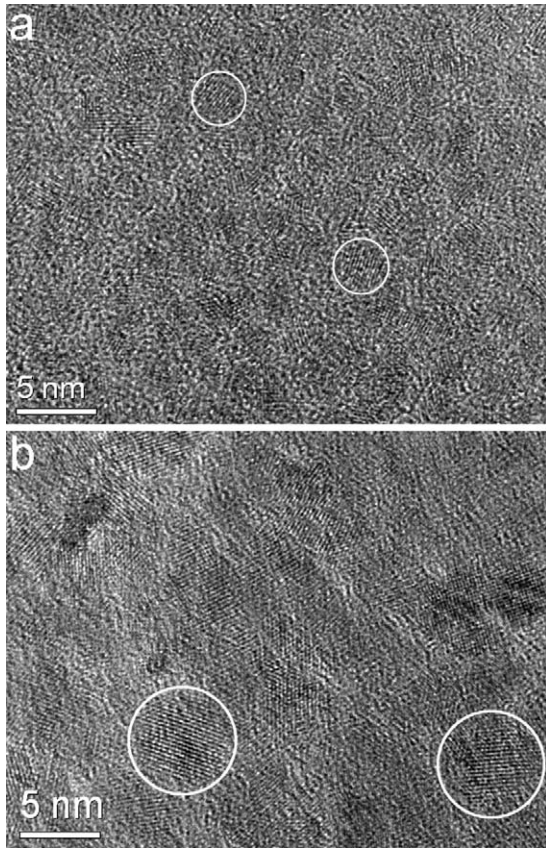
Fig. 2. HR-TEM micrographs showing evenly distributed and well separated TiC nanograins in the nanocomposite coatings: (a) H3 and (b) H5.

coatings H2, H3 and H5 are still very small, just a couple of hundred nanometer longer than the corresponding median cracks of several micrometers in size (see Fig. 3a). Rather, no radial crack may be induced even at such a high load on the coating H4 and H6, as shown in Fig. 3b. Further increasing the indentation load makes the coatings to spall off due to failure in the Si-wafer underneath. Meanwhile, SEM observations on the indentation impressions clearly show that the radial cracks propagate readily through the columnar boundaries and leave a long meandering crack path in the coating H5 as seen in Fig. 3c. In contrast, the radial cracks are straight in the coating H3 where columnar structures are restrained (Fig. 3d).

Because the size of the radial cracks measured on the nanocomposite coatings is dominated by the median crack sizes that are inversely proportional to the indentation hardness of the coatings, a compensation of coating hardness is needed when applying Lawn–Evans–Marshall's approach to estimate the fracture toughness in this case. Accordingly, the fracture toughness has been recorded at the value of 49.94 MPa m$^{1/2}$ on the coating H4 and 55.78 MPa m$^{1/2}$ on H6, compared with 23.66 MPa m$^{1/2}$ on H2 and 32.21 MPa m$^{1/2}$ on H5. Even though the recorded toughness figures are unrealistically high, they can serve as an indication of the relative values of the toughness among the nanocomposite coatings.

It is clear that the coatings with a glassy microstructure such as H4 and H6 exhibit substantial toughening effects. To support this comparison, the critical indentation loads (L_r) at which the radial cracks start to propagate are presented in Table 1. Indeed, there is a close correspondence between the toughness and the critical indentation loads. Similarly, the ratio of elastic work to the total work during indentations, W_e/W_t, defined by the areas under the loading and unloading curves of the nanoindentations, respectively, are also relevant to this comparison as listed in Table 1.

Ball-on-disc tribo-tests have been systematically performed on the nanocomposite coatings with Ø 6 mm balls. Three different kinds of friction behavior of the nanocomposite coatings have been distinguished as seen in Fig. 4a. The coating H1 exhibits a nearly constant friction coefficient and the coating H5 shows large fluctuations in the friction coefficient curve. The mean friction coefficient of the coatings H1 and H5 is above 0.2, i.e. much higher than that of the coating H3. The most attractive results are the third mode observed on the coatings H3, H4 and H6 that show not only a low steady-state coefficient of friction (CoF) but also a continuous drop of the friction until the steady-state is reached. Such a behavior is attributed to the gradual formation of a transfer film on the counterpart surface during the early stage of a tribo-test, which makes the contact in between two basically similar hydrophobic a-C:H surfaces that exhibit self-lubrication effects. However, if the a-C(:H) matrix cannot efficiently shield the TiC particles in the transfer films as in the cases of nanocomposite coatings with a high volumetric fraction of (rather big) TiC nanocrystallites, TiC nanoparticles may cause considerable damage to the hydrophobic contact surfaces. This may explain the fluctuations in the friction graph of H5 as shown in Fig. 4a.

The tribological sensitivity of the nanocomposite coatings to the environments, namely different atmosphere and humidity, has been examined as well. At a low humidity of 25 ± 1% achieved by flowing dry nitrogen in the testing chamber at least for 45 min before testing, the wear tests have registered a very high CoF (0.562) between the coating H6 and fresh uncoated steel balls, as shown in Fig. 4b. Such a high value of CoF appears to be not simply due to the lower humidity alone, but rather a tribochemical reaction between the contacting surfaces with the mixed atmosphere of nitrogen and water molecules. Further tribo-tests have shown that changes in relative humidity by flowing dry air into the testing chamber leads to only a gradual increase in the CoF, e.g. 0.018, 0.021 and 0.069 at the relative humidity of 0%, 25% and 50%, respectively. However, if transfer films are first formed on the surface of the steel ball by wear testing in ambient air as usual, successive wear testing in nitrogen, i.e. at 25% humidity leads to an ultra-low friction with a coefficient of about 0.012. Especially when the atmosphere is cycled between ambient air and nitrogen, the transitions from low to ultralow friction and the reverse are repeatedly switchable, as demonstrated in Fig. 4b. On the other hand, it is difficult to build up
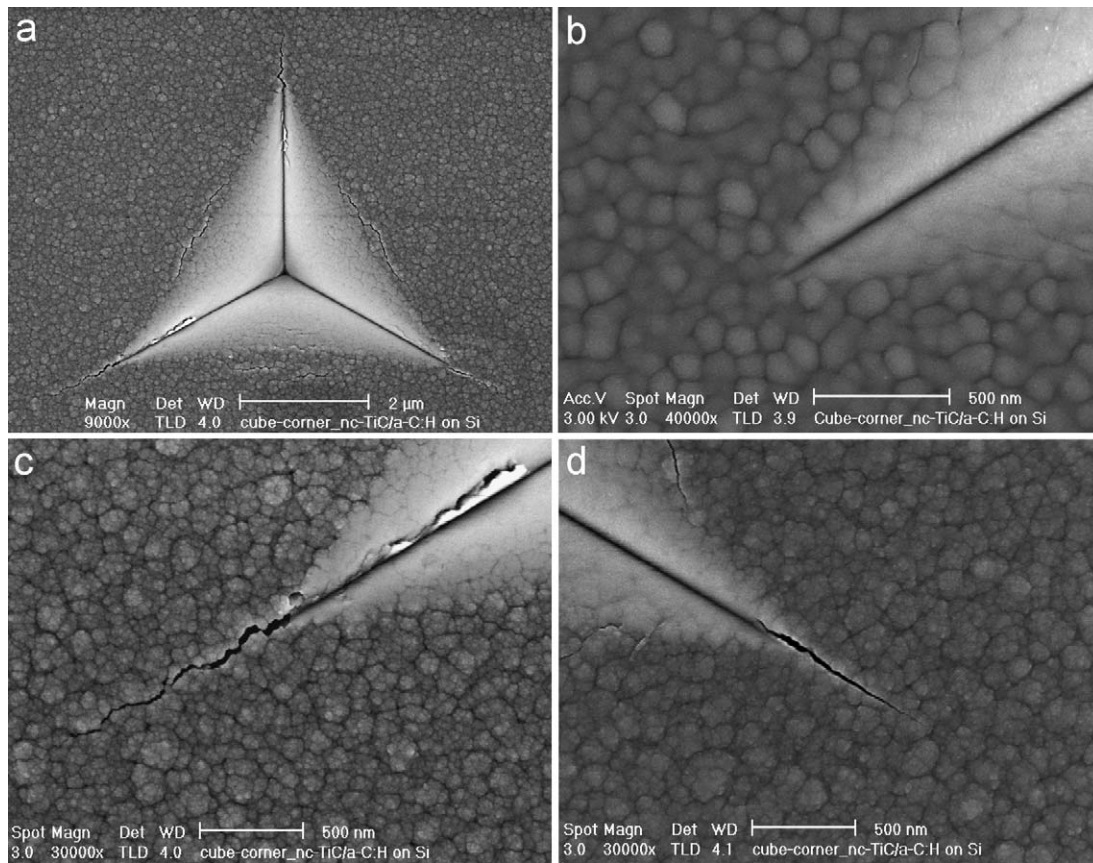
Fig. 3. SEM micrographs showing the nanoindentation impressions made with a cube-corner indenter on the coatings (maximum indentation load 190 mN): (a) H5 and (b) H4. Magnified micrographs (c) and (d) showing the path of radial cracks on the coating H5 and H3, respectively.

transfer films under ultralow friction and instead, the transfer films may be locally worn out from the ball surface if the coating is rather hard. As a consequence, the state of ultralow friction may be broken down after a long period of sliding.

Such a behavior has been observed on the coating H4 (Fig. 4c) where the self-lubrication vanishes after 3200 laps running under ultralow friction, even though the coating is still not penetrated.

Table 2
Tribo-test parameters and wear rate of nc-TiC/a-C nanocomposite coatings at room temperature

| Coating	Load (N)	Laps (n)	Ø 6 mm ball	Atmosphere	Humidity (%)	Steady-state COF, μ	Wear rate [$\times 10^{-15}$ m^3/N m lap]
H1	2	12545	100Cr6	Air	50	0.290	2.2
	5	10630	100Cr6	Air	51	0.280	1.4
H2	2	25000	100Cr6	Air	46	0.062	0.0702
	5	10000	100Cr6	Air	50	0.069	0.1609
H3	2	25000	Al$_2$O$_3$	Air	45	0.076	0.049
	2	12500	100Cr6	Air	46	0.062	0.048
	5	5000	100Cr6	Air	45	0.046	0.089
H4	5	761	100Cr6	N$_2$	25	0.701	18.92
	2	40000	100Cr6	Air	45	0.073	0.0303
	5	10000	100Cr6	Air	47	0.090	0.0517
	5	10000	100Cr6	Vapor	74	0.087	0.0179
H5	2	12000	Al$_2$O$_3$	Air	46	0.387	2.8
	2	12500	100Cr6	Air	46	0.280	3.1
	5	5000	100Cr6	Air	45	0.244	1.8
H6	5	559	100Cr6	N$_2$	25	0.562	10.24
	5	10000	100Cr6	Air	50	0.069	0.0306
	5	10000	100Cr6	Vapor	75	0.092	0.0131
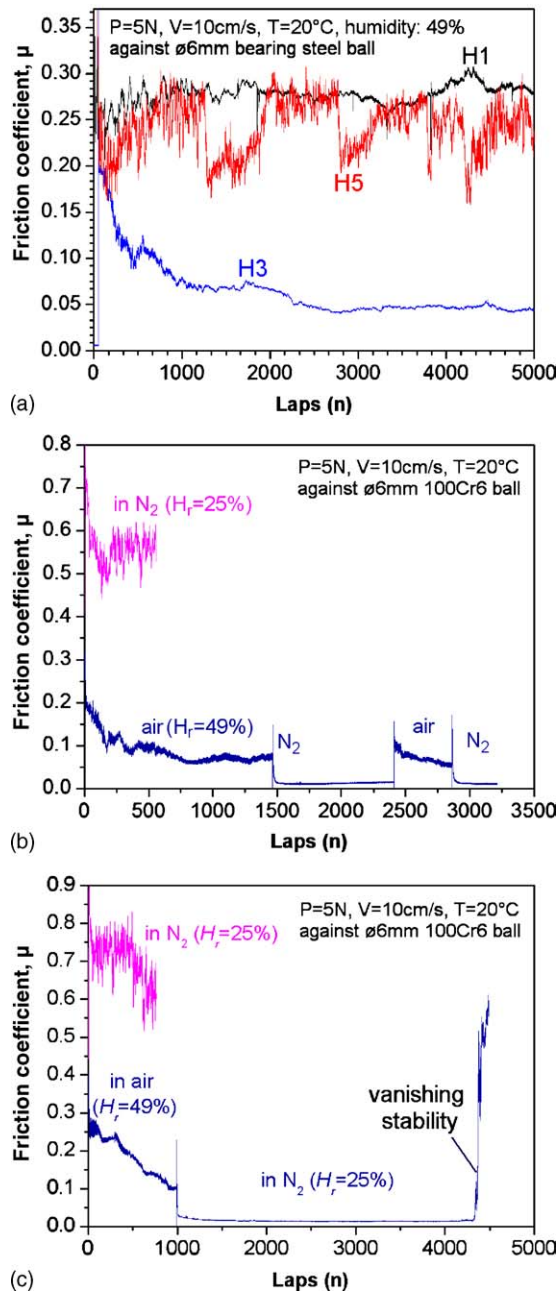
Fig. 4. Friction coefficient graphs of nc-TiC/a-C:H nanocomposite coatings: (a) three characteristic friction behaviors observed on the coating H1, H3 and H5, respectively; effects of relative humidity and atmospheres on the friction behavior of the coating H6 (b) and H4 (c) tested directly in humid nitrogen and in air-nitrogen cyclic atmosphere, respectively.

The tribo-test results of all the coatings are summarized in Table 2. It is clear that the wear rate of the nanocomposite coatings significantly decreases with increase in hardness and especially with increasing the H/E ratio. In general, the wear rate rises if a higher normal load is applied, which is simply related to the higher contact stresses. Changing the counterpart from bearing steel to alumina ball has almost no influence on the wear rate. In contrast, the relative humidity and atmosphere dramatically affect the wear properties,

including both the friction coefficient and the wear rate. The wear rate in humid nitrogen is three orders of magnitude higher than the one in air. After several hundreds laps of sliding, the coatings tested directly in humid nitrogen have already worn out through the entire thickness. The lowest wear rate of 1.31×10^{-17} m^3/(N m lap) is achieved on the coating H6 tested in 75% relative humidity.

4. Conclusions

TiC/a-C:H nanocomposite coatings are composed of TiC nanocrystallites separated by amorphous hydrocarbon matrix. The columnar growth of the coatings can be restrained by increasing substrate bias or carbon content, which is crucial for obtaining high toughness and resistance against surface fatigue. Superior wear resistance is achieved on the coatings with a high H/E ratio and strong self-lubrication effects. These coatings also exhibit ultralow friction when tested in low humidity/N$_2$ atmosphere, and especially, the transitions from low to ultralow friction and the reverse are repeatedly switchable if the atmosphere is cycled between ambient air and nitrogen. The lowest wear rate is obtained at high humidity.

References

1. Pei, Y. T., Galvan, D. and De Hosson, J. Th. M., Nanostructure and properties of TiC/a-C:H composite coatings. *Acta Mater.*, 2005, in press.
2. Meng, W. J. and Gillispie, B. A., Mechanical properties of Ti-containing and W-containing diamond-like carbon coatings. *J. Appl. Phys.*, 1998, **84**, 4314–4321.
3. Meng, W. J., Tittsworth, R. C. and Rehn, L. E., Mechanical properties and microstructure of TiC/amorphous hydrocarbon nanocomposite coatings. *Thin Solid Films*, 2000, **377–378**, 222–232.
4. Strondl, C., Carvalho, N. M., De Hosson, J. Th. M. and Van der Kolk, G. J., Investigation on the formation of tungsten carbide in tungsten-containing diamond like carbon coatings. *Surf. Coat. Technol.*, 2003, **162**, 288–293.
5. Pharr, G. M., Measurement of mechanical properties by ultra-low load indentation. *Mater. Sci. Eng. A*, 1998, **A253**, 151–159.
6. Lawn, B. R., Evans, A. G. and Marshall, D. B., Elastic/plastic indentation damage in ceramics: the median/radial crack system. *J. Am. Ceram. Soc.*, 1980, **63**, 574–581.
7. Pei, Y. T., Galvan, D., De Hosson, J. Th. M. and Cavaleiro, A., Nanostructured TiC/a-C coatings for low friction and wear resistant applications. *Surf. Coat. Technol.*, 2005, **198**, 44–50.
8. Leyland, A. and Matthews, A., On the significance of the H/E ratio in wear control: a nanocomposite coating approach to optimised tribological behaviour. *Wear*, 2000, **246**, 1–11.